

MORPHOLOGY AND DEVELOPMENT OF HATCHERY-CULTURED AMERICAN SHAD, *ALOSA SAPIDISSIMA* (WILSON)¹

JAMES R. JOHNSON² AND JOSEPH G. LOESCH³

ABSTRACT

Morphometrics and meristics of larval *Alosa sapidissima* (Wilson) were examined and are described for hatchery-reared samples. *Alosa sapidissima* morphometrics and body proportion ratios change with ontogeny in the larval stages. Head and snout length, eye diameter, and body depth exhibit a curvilinear relationship with increasing standard length, while preanal and predorsal length show a linear relationship with increasing standard length.

Predorsal and preanal myomere counts decrease during ontogeny with corresponding anterior dorsal fin migration and shortening of the gut. Other meristics indicate that median fin development is completed between 17 and 21 mm SL, while paired fin development is completed between 23 and 28 mm SL. A developmental sequence of the various caudal fin components shows a distinction between preflexion, flexion, and postflexion larvae. The developments of hypurals and notochord flexure are important in distinguishing larval and early juvenile stages of development.

Pigmentation shows a greater number and density of melanophores on cultured than field-sampled specimens. Stellate melanophores are found to contract and migrate on cultured samples. A sequence of pigmentation changes with ontogeny is described and compared with two sympatric species.

The American shad, *Alosa sapidissima* (Wilson), is a commercially and recreationally important clupeid commonly found in western North Atlantic coastal waters from Newfoundland, Canada, to the St. Johns River, Fla. (Hildebrand 1963; Scott and Crossman 1973; Chittenden 1969; Leim 1924; Watson 1968). Life history studies of *A. sapidissima* have been limited primarily to the juvenile and adult stages of development (Carscadden and Leggett 1975; Chittenden 1969; Leim 1924).

The sequence of egg development for *A. sapidissima* has been adequately described by Hildebrand (1963), Watson (1968), and Marcy (1976). Leim (1924) described yolk-sac larvae and field-sampled larvae up to 28 mm in length. Hildebrand (1963) described yolk-sac larvae and briefly described the larval development through the juvenile stage. Mansueti and Hardy (1967), Lippson and Moran (1974), and Jones et al. (1978) all summarized the early development of *A. sapidissima*. The approach previously used to describe *A. sapidissima* appears to

be the static technique, which describes a few larvae over selected or sampled size ranges.

This paper describes the development of *A. sapidissima* from yolk absorption through the juvenile stage of development, using the dynamic description approach of Moser and Ahlstrom (1970). Special attention is given in this work to morphology, meristics, and pigmentation; early caudal osteology is examined from sequential samples and a sequence of ossification is also described.

METHODS

Eggs were cultured in a flow-through system designed by Blair (1976). Apparatus used in the system included three to five 10-l culture jars. A constant flow rate was maintained into an open trough of running water. The trough contained specially designed baskets fitted with saran screen for holding the newly hatched *A. sapidissima*. Larvae were sequentially sampled daily for the first 30 d, then weekly until the end of a 100-d sampling period. Samples were preserved by the method recommended by Berry and Richards (1973), in 10% buffered Formalin⁴.

Two developmental series of larvae were used. Specimens in the first series were used for morphometric data, pigment patterns, and larval il-

¹Contribution No. 1074, School of Marine Science, Virginia Institute of Marine Science, College of William and Mary, Gloucester Point, Va.

²Department of Ichthyology, School of Marine Science, Virginia Institute of Marine Science, College of William and Mary, Gloucester, Va.; present address: Environmental Affairs Department, Rio Blanco Oil Shale Company, 2851 S. Parker Road, Suite 500, Aurora, CO 80014.

³Department of Ichthyology, School of Marine Science, Virginia Institute of Marine Science, College of William and Mary, Gloucester Point, VA 23062.

⁴Reference to trade names does not imply endorsement by the National Marine Fisheries Service, NOAA.

illustrations. Those in the second series were cleared and counterstained by the method used by Dingerkus and Uhler (1977) for meristic and caudal osteology studies. Selected specimens in the first series were subsequently used for staining in the second series, after measurements, pigment patterns, and illustrations were completed. Field specimens of *A. sapidissima* were also examined by the counterstaining technique.

Morphometrics were taken by using an ocular micrometer, calibrated to the nearest 0.1 mm, in a dissecting microscope and a dial caliper, calibrated to the nearest 0.1 mm. Measurements follow closely those of Houde et al. (1974) and are described as follows:

Total Length (TL): Tip of snout to end of caudal finfold complex in yolk sac and preflexion larvae, and to end of the longest superior procurrent caudal ray in flexion and postflexion larvae.

Notochord-Standard Length (SL): Tip of snout to tip of notochord in yolk sac, preflexion, and early flexion larvae; tip of snout to base of hypural plate in flexion and late flexion larvae; and tip of snout to the point midway between the tenth superior procurrent caudal ray and the first inferior caudal ray in postflexion larvae and juveniles. Unless otherwise noted in the text, all references to lengths of larvae refer to standard lengths. The use of this criteria for standard length measurements is based on that set forth by Richards et al. (1974).

Preanal Length (PAL): Tip of snout to end of anus measured along the midline of the body. This measurement is also used to describe the location of the anal fin for specimens that have shown development of the anal fin complex.

Predorsal Length (PDL): Tip of snout to break in finfold for specimens in yolk sac or very early preflexion stage of development; tip of snout to origin of first dorsal ray measured along the midline of the body for fish exhibiting dorsal fin development. If dorsal rays were not evident, then measurement was made at the origin of the first dorsal radial bone.

Head Length (HL): Tip of snout to posterior margin of auditory vesicle in yolk sac and early preflexion larvae; tip of snout to posterior margin of opercular membrane and bone when development was evident.

Eye Diameter (HED): Horizontal diameter between anterior and posterior edges of the fleshy orbit.

Snout Length (SNTL): Tip of snout to anterior margin of fleshy orbit on the eye.

Body Depth (BD): Vertical height of the body measured at origin of the first dorsal ray.

All morphometrics were taken on the left side of the fish body. Damaged specimens were not used; doubtful measurements were eliminated from the study. Meristics were taken from cleared and counterstained flexion and postflexion specimens per the methods of Berry and Richards (1973).

RESULTS

Morphology of Larvae

Morphometrics for larval *A. sapidissima* are presented in Table 1. *Alosa sapidissima* body proportions change during ontogeny with the most abrupt changes occurring between 12 and 18 mm SL. HL, SNTL, HED, and BD all exhibit curvilinear growth with increasing SL. PAL and PDL exhibit linear growth with increasing SL.

SL was used to examine development of *A. sapidissima* with respect to the other morphometric data. Inspection of Figure 1 and a high coefficient of determination ($r^2 = 0.998$) indicate a strong linear relationship. SL length fluctuated between 97.5 and 92.4% of the TL for larvae measured. There were no changes in the TL and SL relationship between 8 and 13 mm, where it remained at 96%. Changes in this relationship were seen in the early postflexion stage of development, between 18 and 23 mm (Table 1), when the SL decreased from 97.2 to 95.7%. The SL/TL ratio averaged 96.5% for larvae <15 mm and 95.5% for larvae 15-31 mm. The decrease in body proportion for the SL/TL relationship is related to caudal fin development, particularly notochord flexure between 12 and 15 mm, along with development of the first and second hypural plates.

PAL exhibited a steady decrease from 95% for 8 mm larvae to 65.4% for 31 mm larvae. Examination of Figure 2, along with a high coefficient of determination ($r^2 = 0.969$), also tends to indicate a linear relationship. At 18 mm SL, where the PAL/SL ratio is invariable, transformation occurs from the flexion to postflexion stage. The major changes in this relationship were seen between 23 and 27 mm TL (Table 1). Over this TL range, the gut is shortened and transformations to the postflexion stage became evident, which tends to account for the decrease in the PAL and SL relationship.

PDL decreased with increasing SL (Table 1). There appear to be three distinct size intervals at which the PDL decreases (Fig. 3). The dorsal fin migrates forward as dorsal rays develop and SL increases. This

TABLE 1.—Morphometrics (in mm) for larval American shad, *Alosa sapidissima*. \bar{x} = Mean; SD = Standard deviation; R = Range; * = Missing values; ** = One value only; TL = Total length; SL = Standard length; PAL = Preanal length; PDL = Predorsal length; PPL = Prepelvic length; HL = Head length; SNTL = Snout length; HED = Horizontal eye diameter; BD = Body depth.

Size (mm)	N	Stat.	TL	SL	PAL	PDL	PPL	HL	SNTL	HED	BD
8	9	\bar{x}	8.64	8.38	7.55	*5.60	—	1.23	0.20	0.36	0.61
		SD	0.174	0.212	0.230	—	—	0.086	0.026	0.033	0.055
		R	8.40-8.90	8.10-8.70	7.25-7.95	—	—	1.15-1.32	0.15-0.23	0.31-0.40	0.51-0.70
9	39	\bar{x}	9.64	9.31	7.65	*6.24	—	1.37	0.20	0.40	0.61
		SD	0.265	0.276	0.201	0.255	—	0.090	0.036	0.047	0.072
		R	9.00-9.99	8.60-9.67	7.13-7.96	5.72-6.60	—	1.17-1.62	0.11-0.25	0.31-0.51	0.43-0.76
10	23	\bar{x}	10.43	10.01	8.12	6.60	—	1.46	0.21	0.46	0.62
		SD	0.360	0.340	0.196	0.152	—	0.114	0.059	0.053	0.109
		R	10.00-10.97	9.50-10.60	7.81-8.57	6.30-6.94	—	1.25-1.71	0.11-0.32	0.33-0.55	0.52-0.83
11	16	\bar{x}	11.36	10.97	8.79	7.09	*5.05	1.64	0.26	0.49	0.70
		SD	0.284	0.298	0.251	0.183	0.566	0.130	0.045	0.031	0.076
		R	11.02-11.72	10.60-11.42	8.41-9.25	6.88-7.38	4.65-5.45	1.40-1.81	0.19-0.36	0.43-0.51	0.58-0.85
12	5	\bar{x}	12.49	12.05	9.52	7.63	**4.97	2.06	0.32	0.50	1.02
		SD	0.242	0.246	0.313	0.287	—	0.073	0.025	0.024	0.018
		R	12.17-12.71	11.78-12.28	9.55-10.28	7.25-8.00	—	1.96-2.10	0.30-0.36	0.46-0.52	1.01-1.05
13	2	\bar{x}	13.51	13.00	10.99	8.25	**5.57	2.34	0.37	0.61	1.26
		SD	0.325	0.707	0.594	1.089	—	0.332	0.099	0.014	0.071
		R	13.28-13.74	12.50-13.50	10.57-11.41	7.48-9.02	—	2.10-2.57	0.30-0.44	0.60-0.62	1.21-1.31
14	2	\bar{x}	14.24	13.65	11.40	8.76	5.58	2.40	0.44	0.71	1.31
		SD	0.042	0.283	0.212	0.509	0.198	0.071	0.035	0.141	0.014
		R	14.21-14.27	13.45-13.85	11.25-11.55	8.40-9.12	5.44-5.72	2.35-2.45	0.41-0.46	0.61-0.81	1.30-1.32
15	2	\bar{x}	15.75	15.34	12.22	8.98	**6.57	2.90	0.54	0.76	**1.54
		SD	0.099	0.148	0.134	0.078	—	0.014	0.085	0.071	—
		R	15.68-15.82	15.23-15.44	12.12-12.31	8.92-9.03	—	2.89-2.91	0.48-0.60	0.71-0.81	—
16	4	\bar{x}	16.46	16.05	12.60	9.20	*6.30	3.00	0.61	0.74	1.74
		SD	0.191	0.130	0.092	0.114	0.445	0.065	0.021	0.045	0.130
		R	16.24-16.63	15.93-16.17	12.50-12.72	9.07-9.31	6.00-6.81	2.96-3.06	0.58-0.63	0.70-0.80	1.62-1.86
17	1	\bar{x}	17.46	16.91	13.55	9.78	7.28	3.02	0.55	0.80	1.88
		SD	—	—	—	—	—	—	—	—	—
		R	—	—	—	—	—	—	—	—	—
18	1	\bar{x}	18.28	17.77	13.58	9.75	7.19	3.57	0.68	1.01	1.96
		SD	—	—	—	—	—	—	—	—	—
		R	—	—	—	—	—	—	—	—	—
20	2	\bar{x}	20.47	19.63	13.96	10.83	8.55	4.25	1.01	1.16	2.46
		SD	0.134	0.417	0.028	0.544	0.382	0.070	0.028	0.064	0.148
		R	20.37-20.56	19.33-19.92	13.94-13.98	10.44-11.21	8.28-8.82	4.20-4.30	0.99-1.03	1.11-1.20	2.35-2.56
21	2	\bar{x}	21.05	19.44	13.56	9.40	—	4.21	1.11	1.33	2.39
		SD	0.071	0.042	0.353	0.332	—	0.056	0.035	0.148	0.028
		R	21.00-21.10	19.41-19.47	13.31-13.81	9.16-9.63	—	4.17-4.25	1.08-1.13	1.22-1.43	2.37-2.41
23	2	\bar{x}	23.26	22.28	15.41	10.43	—	4.91	1.26	1.73	3.80
		SD	0.127	0.537	0.290	0.184	—	0.276	0.226	0.184	0.163
		R	23.17-23.35	21.91-22.66	15.20-15.61	10.30-10.56	—	4.71-5.10	1.11-1.42	1.60-1.86	3.68-3.91
24	1	\bar{x}	24.28	23.13	15.00	11.41	—	5.62	1.33	1.75	4.04
		SD	—	—	—	—	—	—	—	—	—
		R	—	—	—	—	—	—	—	—	—
25	3	\bar{x}	25.24	23.98	15.01	10.20	**10.08	5.83	1.43	2.15	5.02
		SD	0.110	0.583	0.775	0.061	—	0.105	0.165	0.165	0.322
		R	25.15-25.36	23.46-24.61	14.15-15.65	10.13-10.25	—	5.73-5.94	1.32-1.62	1.96-2.26	4.68-5.32
27	1	\bar{x}	27.05	25.76	16.94	11.88	**11.63	6.76	1.83	2.07	5.39
		SD	—	—	—	—	—	—	—	—	—
		R	—	—	—	—	—	—	—	—	—
28	3	\bar{x}	28.34	26.61	17.39	12.60	12.46	6.76	1.78	1.99	5.37
		SD	0.104	0.079	0.371	0.051	0.157	0.157	0.090	0.055	0.570
		R	28.27-28.46	26.52-26.67	16.99-17.72	12.54-12.64	12.28-12.57	6.64-6.94	1.73-1.88	1.94-2.05	4.83-5.97
29	2	\bar{x}	29.54	28.17	18.57	12.22	12.17	6.61	1.55	1.86	5.46
		SD	0.445	0.487	0.375	0.430	0.410	0.156	0.071	0.198	0.156
		R	29.22-29.85	27.82-28.51	18.30-18.83	11.93-12.50	11.88-12.46	6.60-6.72	1.50-1.60	1.72-2.00	5.35-5.57
30	1	\bar{x}	30.93	29.50	19.50	**12.91	12.60	6.65	1.99	2.11	5.90
		SD	—	—	—	—	—	—	—	—	—
		R	—	—	—	—	—	—	—	—	—
31	1	\bar{x}	31.25	29.66	19.55	**12.93	12.68	8.15	2.12	2.64	6.38
		SD	—	—	—	—	—	—	—	—	—
		R	—	—	—	—	—	—	—	—	—
Total	122										

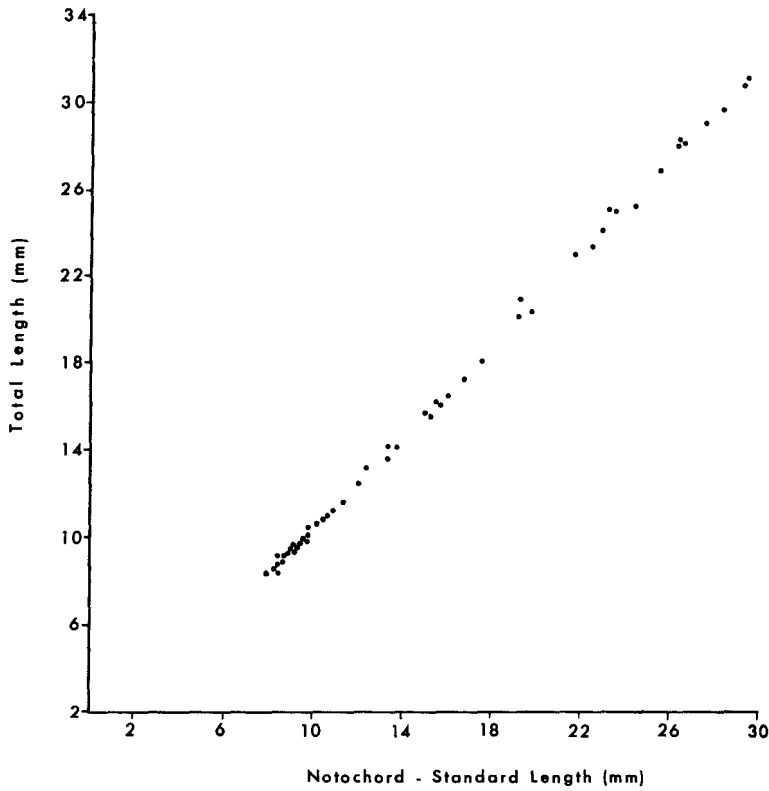


FIGURE 1.—Scatterplot of TL/SL for larval *Alosa sapidissima*. Regression equation:
 $TL = -0.30 + 1.06 SL; r^2 = 0.998$.

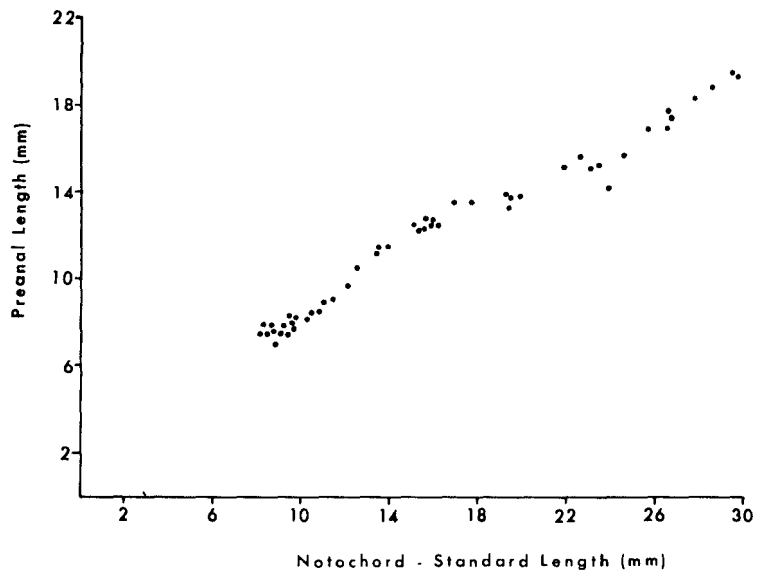


FIGURE 2.—Scatterplot of PAL/SL for larval *Alosa sapidissima*. Regression equation:
 $PAL = 2.18 + 0.60 SL; r^2 = 0.969$.

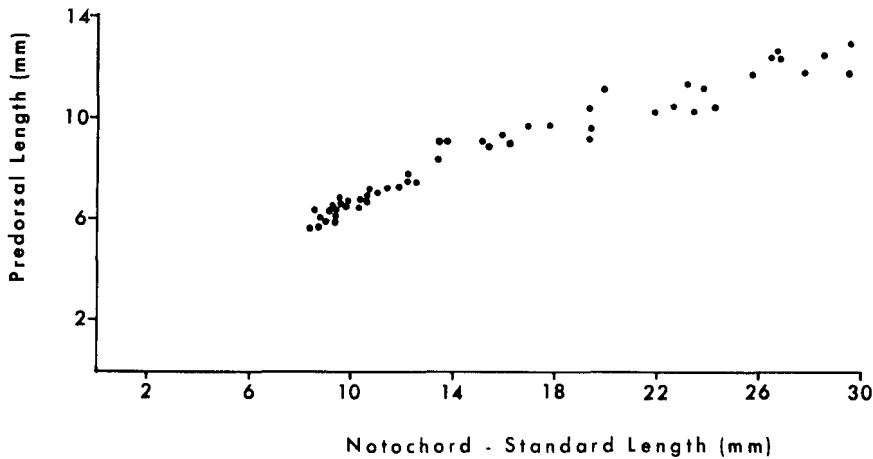


FIGURE 3.—Scatterplot of PDL/SL for larval *Alosa sapidissima*. Regression equation:
 $PAL = 2.62 + 0.39SL; r^2 = 0.964$.

accounts for the decrease in predorsal body proportions from 66.7 to 43.6% of the SL. This decrease is reported to be common for clupeoid larvae (Ahlstrom 1968; Houde et al. 1974; Jones et al. 1978).

Larvae of *A. sapidissima* are relatively big-headed in comparison to their thin nonrobust body in the preflexion and flexion stages. Head development is prominent in larvae between 8 and 11 mm. Five branchial arches, jaws, and two pairs of recurved teeth in the lower jaw were also evident in larvae this size. HL averages 14.7% of SL between 8 and 11 mm (Table 1). At 12 mm, HL increases to 17.0% of SL. An increase of 1.2% is evident in the HL/SL relationship

for larvae 12-17 mm. HL increases from 20.1 to 27.5% of SL in larvae 18-31 mm.

The HL/SL relationship is not as obvious in late flexion and postflexion larvae because the body has become more robust. Examination of Figure 4 at first tends to indicate a linear relationship between HL and SL. However, there appears to be a point in Figure 4 at the transformation between the flexion and postflexion stages (18 mm SL) where the HL/SL relationship may exhibit allometric growth. Fitting the data to the model for an allometric growth curve (Sokal and Rohlf 1969) produced a higher coefficient of determination ($r^2 = 0.992$). Thus the HL/SL ratio

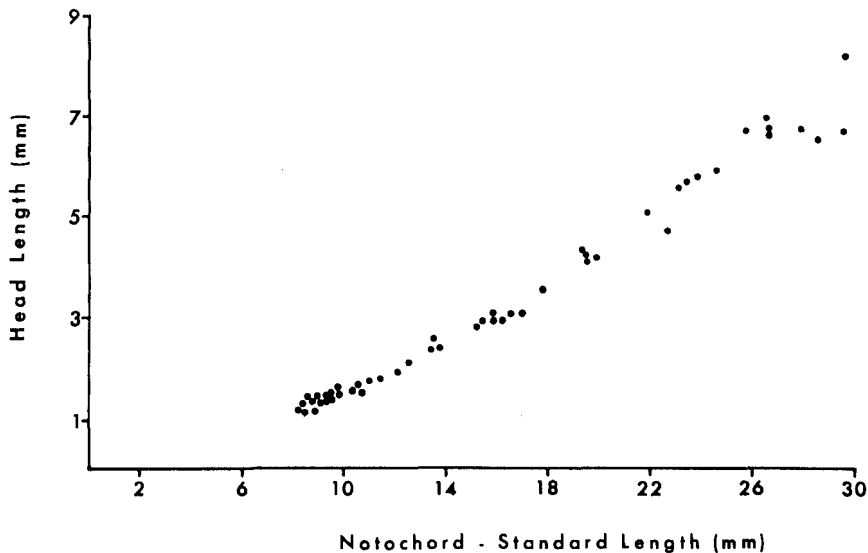


FIGURE 4.—Scatterplot of HL/SL for larval *Alosa sapidissima*. Regression equation:
 $\ln(HL) = \ln 0.05 + 1.50 \ln(SL); r^2 = 0.992$.

probably exhibits a positively allometric relationship.

HED shows an allometric growth relationship with SL. Both HED and SL were log-transformed to fit the linear regression of these two morphometric variables (Fig. 5). HED are variable for a given size interval; at 23 mm SL they vary between 1.60 and 1.86 mm, and at 29 mm SL between 1.72 and 2.00 mm (Fig. 5). Most of the variability occurs between 19 and 31 mm SL, after the transformation from flexion to postflexion larvae. Very little variation occurs in the preflexion and flexion stages (6-18 mm SL).

SNTL appears to exhibit allometric growth with respect to SL (Fig. 6). Both SNTL and SL were log-transformed to fit a linear relationship between these two variables. Snout lengths are variable for a given size range in the postflexion stage, while very little variation occurs within individual size ranges between 6 and 18 mm SL (Fig. 6).

BD exhibits allometric growth with respect to SL (Fig. 7). Increases in BD indicate corresponding increases in body weight and body volume. As the SL and BD increase, the body shape becomes more streamlined, changing from a thin rodlike shape to a deep-bodied, streamlined shape in *A. sapidissima*.

Myomeres

Myomere counts have been shown to be useful for identifying clupeoid genera (Ahlstrom 1968; Houde et al. 1974). The total number of myomeres ranged from 54 to 58; most of the larvae had 55 or 56 myomeres. The number and distribution of myomeres relative to body morphology are shown in Table 2.

The distribution of myomeres was examined in relation to predorsal and preanal body measurements. Predorsal myomeres decreased in number with increasing SL. Predorsal myomere counts decreased

TABLE 2.—Distribution of myomeres relative to other body morphology for *Alosa sapidissima* larvae. *N* = Number of specimens counted; \bar{x} = Mean myomere counts; R = Range of myomere counts.

Size interval (mm SL)	Preanal myomeres			Postanal myomeres			Predorsal myomeres		
	<i>N</i>	\bar{x}	R	<i>N</i>	\bar{x}	R	<i>N</i>	\bar{x}	R
8.0-9.0	11	48.4	45-52	9	12.3	10-14	11	33.9	31-36
9.1-12.0	18	46.1	43-51	17	11.6	10-14	18	30.7	28-35
12.1-15.0	9	44.4	42-48	7	14.6	11-16	9	28.5	26-33
15.1-18.0	7	41.3	39-43	7	15.6	13-17	7	23.3	21-26
18.1-21.0	3	39.0	36-42	—	—	—	3	22.6	21-24
21.1-24.0	4	38.5	35-43	—	—	—	4	21.0	20-23

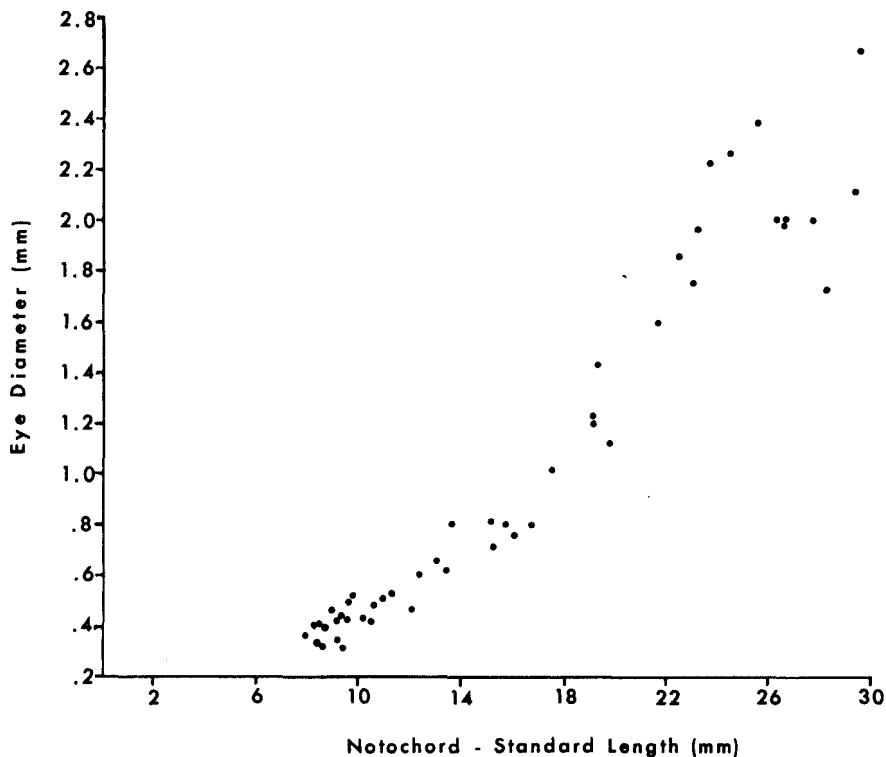


FIGURE 5.—Scatterplot of HED/SL for larval *Alosa sapidissima*. Regression equation: $\ln(\text{HED}) = \ln 0.01 + 1.59 \ln(\text{SL}); r^2 = 0.973$.

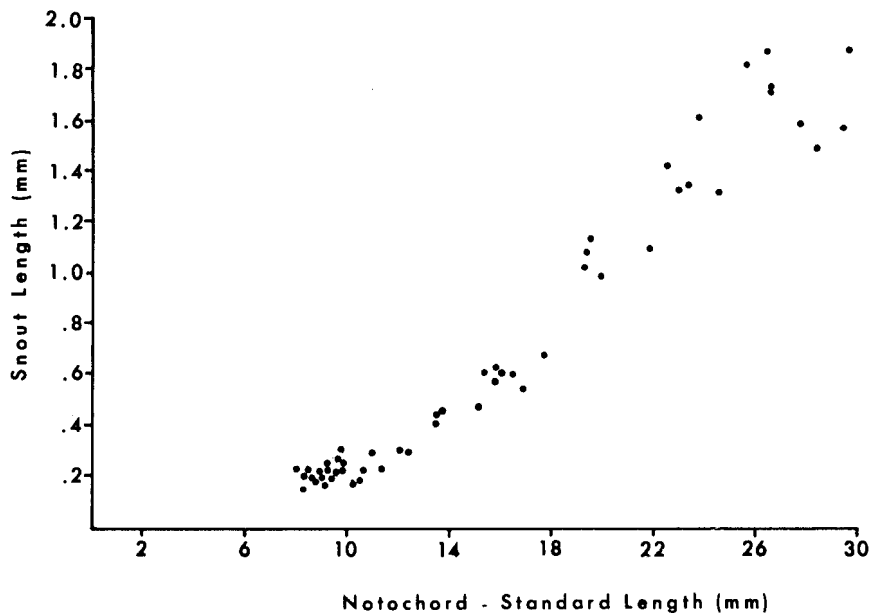


FIGURE 6.—Scatterplot of TL/SL for larval *Alosa sapidissima*. Regression equation:
 $\ln(\text{SNTL}) = \ln 2.31 + 2.01 \ln(\text{SL}); r^2 = 0.964$.

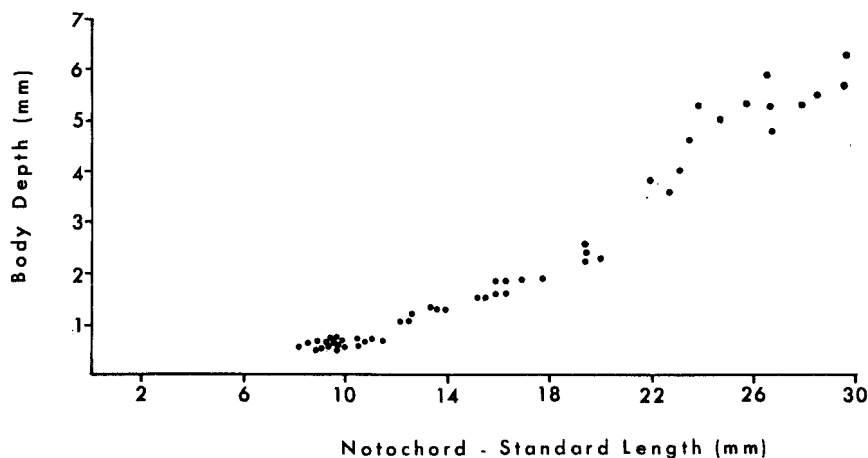


FIGURE 7.—Scatterplot of BD/SL for larval *Alosa sapidissima*. Regression equation:
 $\ln(\text{BD}) = \ln 4.91 \ln + 2.14 \ln(\text{SL}); r^2 = 0.977$.

from a mean of 33.9-21.0 for the larvae examined ($N = 52$). Significant changes in predorsal myomere counts were seen in the 12.1-18.0 mm SL size interval (Table 2). There is, however, considerable variation in predorsal myomere counts for all size intervals, as shown in Table 2.

Counts for preanal myomeres decreased with increasing SL and decreasing PAL. There was a decrease in the mean number of preanal myomeres from 48.4 to 38.5 for the larvae examined. This de-

crease parallels the shortening of the gut as the SL increases.

The mean number of postanal myomeres increased with the shortening of the gut and increasing SL. An increase from a mean of 12.3 to 15.6 postanal myomeres was evident for the larvae examined ($N = 40$; Table 2). No information is available in this study for postanal myomere counts in larval *A. sapidissima* >18.0 mm SL.

Fin Development

Median and paired fin development is indicated in Tables 3 and 4 for both hatchery-cultured and field-sampled specimens. A summary of the fin development of cultured specimens is presented in Table 5. Development of the median fins (dorsal, anal, and caudal), including ossification of rays, is first evident between 9.0 and 12.5 mm SL. Median fin development is completed between 17 and 21 mm SL. Paired fin development is not truly evident until larvae are in the late flexion or early postflexion stages. Development of the paired fins was complete when larvae were between 23 and 27 mm SL (Table 5).

The dorsal fin exhibits the earliest development of all fins. Dorsal fin radials first appear in larvae 8.0-9.0 mm SL (Table 5). Radials appear as buds and are not fully developed at this stage.

The developmental sequence for the various components of the caudal complex is described from the

first appearance of cartilaginous structures to a gradual ossification and fusion of bones in the caudal complex. The criteria used to place larvae into one of the three larval stages of development are similar to that described by Tucker (1978). Description of the sequence of caudal complex development is based on 19 selected counterstained specimens (Figs. 8, 9).

Larvae between hatch and 9.5 mm SL had a straight notochord (no flexure) and showed no evidence of any support structure development (hypurals, uro-neurals, neural, or haemal spines) (Fig. 8A). Early caudal fin development is evident in the late preflexion stage in larvae 9.8-11.3 mm SL. The notochord is straight, and one incipient parhypural and one to three incipient hypurals have begun to develop (Fig. 8B). The hypurals and parhypural first appear stained with Alcian Blue. There is some incipient caudal fin ray development (Table 3).

Notochord flexure starts between 11.5 and 12.6 mm

TABLE 3.—Some fin meristics for larval *Alosa sapidissima* cultured at USFWS Harrison Lake National Fish Hatchery, Va.

Notochord standard length (mm)	Dorsal rays	Anal rays	Pectoral rays	Pelvic rays	Caudal rays			
					Superior procurent	Superior principal	Inferior principal	Inferior procurent
Preflexion larvae								
9.25	8	—	—	—	—	—	—	—
9.59	7	—	—	—	—	—	—	—
9.91	8	—	—	—	—	—	—	—
10.00	8	—	—	—	—	—	—	—
10.40	9	—	—	—	—	—	—	—
10.72	9	—	—	—	—	—	—	—
10.85	10	—	—	—	—	—	—	—
11.00	9	—	—	—	—	—	—	—
11.17	9	—	—	—	—	—	—	—
11.42	10	—	—	—	—	2	—	—
11.81	12	3	—	—	—	2	—	—
Flexion larvae								
12.12	12	—	—	—	1	2	2	2
12.28	13	—	—	—	2	4	2	2
12.50	13	8	—	—	4	7	4	—
13.45	15	9	—	—	4	9	5	2
13.50	14	—	—	—	3	9	3	3
13.85	16	12	3	—	—	9	—	—
15.44	17	15	—	—	—	10	4	4
15.93	17	19	—	—	3	10	4	5
15.94	16	8	—	—	—	10	—	—
16.15	18	9	5	—	—	10	4	4
16.17	17	—	2	—	—	10	4	4
16.91	17	17	3	—	5	10	7	—
17.77	18	15	—	—	7	10	5	5
Postflexion larvae								
19.33	18	20	—	4	7	10	7	6
19.41	18	19	8	—	5	10	5	6
19.47	18	18	10	—	8	10	9	7
19.92	17	20	13	6	8	10	9	6
21.66	18	21	—	—	7	10	9	7
21.91	18	19	—	—	8	10	9	7
23.13	19	19	11	—	8	10	9	7
23.46	19	20	—	—	8	10	9	7
24.81	19	22	15	—	8	10	9	7
25.76	19	23	15	8	8	10	9	7
26.52	19	22	16	7	8	10	9	6
26.64	19	22	14	7	8	10	9	7
26.67	19	21	16	8	8	10	9	7
27.82	19	20	16	9	8	10	9	6
28.51	19	19	16	9	8	10	9	7
29.50	19	23	15	10	8	10	9	7

TABLE 4.—Fin development meristics for postflexion (juvenile) *Alosa sapidissima*.

Standard length (mm)	Dorsal rays	Anal rays	Pectoral rays	Pelvic rays	Caudal rays			
					Superior procurrent	Superior principal	Inferior principal	Inferior procurrent
26.5	19	22	15	9	8	10	9	6
26.8	18	23	14	9	8	10	9	7
27.4	18	23	15	9	8	10	9	7
28.2	19	22	16	9	8	10	9	7
28.4	19	22	18	9	8	10	9	6
28.5	19	22	17	9	7	10	9	6
28.6	17	23	17	10	7	10	9	7
28.8	18	23	17	8	7	10	9	6
29.0	17	—	17	9	8	10	9	7
29.1	18	22	14	8	7	10	9	7
29.2	17	21	18	9	7	10	9	7
29.3	18	20	14	8	8	10	9	7
29.5	19	23	15	9	8	10	9	6
29.6	19	23	17	10	8	10	9	7
30.2	21	19	16	8	7	10	9	7
30.4	17	24	16	8	8	10	9	7
31.7	18	21	14	8	8	10	9	7
31.8	18	22	15	9	8	10	9	7
31.8	18	22	15	9	7	10	9	7
32.2	18	21	18	9	7	10	9	6
32.4	19	20	15	11	8	10	9	7
32.9	17	23	15	8	8	10	9	7
33.0	17	21	16	10	7	10	9	6
33.4	17	20	17	8	7	10	9	6
36.2	18	21	18	8	8	10	9	7
37.2	18	23	16	9	8	10	9	7
37.8	18	22	17	10	7	10	9	6
38.4	17	22	14	10	7	10	9	7

TABLE 5.—Summary of fin development sequence in larvae of *Alosa sapidissima* (Wilson).

Fin	Standard length ^{1,2}			
	Buds first appear ³	Rays first appear	Full complement of rays	No. rays in fully developed fins
Dorsal	8.0- 9.0	9.0- 9.3	17.0-20.0	17-20
Anal	11.0-11.7	11.8-12.5	19.0-21.0	19-23
Pectoral	*	13.8-19.4	23.8-25.7	14-18
Pelvic	17.0-19.0	19.0-20.0	25.0-27.0	8-10
Caudal				
Superior procurrent	—	12.0-12.5	19.0-20.0	7-8
Superior principal	—	11.0-12.0	15.0-15.5	10
Inferior principal	—	12.0-12.5	19.0-19.5	9
Inferior procurrent	—	12.0-12.5	19.0-20.0	6-7

¹Rays were present but not necessarily ossified.

²Rays were stained blue or red for counting. (Blue = cartilaginous; Red = ossified bone.)

³Includes the radial and basipterygium bones.

*Incipient rays are evident in yolk-sac larvae, but do not stain with Alcian Blue or Alizarin Red S.

SL, and is completed by 18 mm SL. A specimen 12.1 mm SL exhibited the following characteristics of early notochord flexure: The posterior end of the notochord was beginning to tip up dorsally; one parhypural and the first four hypurals were formed; the anterior portion of the first, second, and third hypurals and parhypural absorbed Alizarin Red S stain, indicating that the structures were ossifying; the fourth hypural and the posterior portion of the first three hypurals and parhypural absorbed Alcian Blue stain; a cartilaginous haemal spine was also evident in this specimen. Another specimen, 13.2 mm SL, exhibited the following characteristics for a larvae in midflexion (Fig. 8C): The posterior end of the

notochord was curved dorsally and then flattened into an S shape; five hypurals were distinct, with hypurals 1, 2, and 3 absorbing Alizarin Red S in the anterior portion of the structure; both haemal and neural spines were present, absorbing both Alcian Blue and Alizarin Red S stains; the first evidence of the first uroneural appeared in this specimen.

Late flexion larval *A. sapidissima* are characterized by complete flexure of the notochord and evidence of segregation into the uroneurals and ural vertebra (Fig. 8D). A cartilaginous sixth hypural plate is also evident. Two slightly fused epural bones are evident, along with the first formation of the neural arch. Both the neural arch and epurals appear as cartilage.

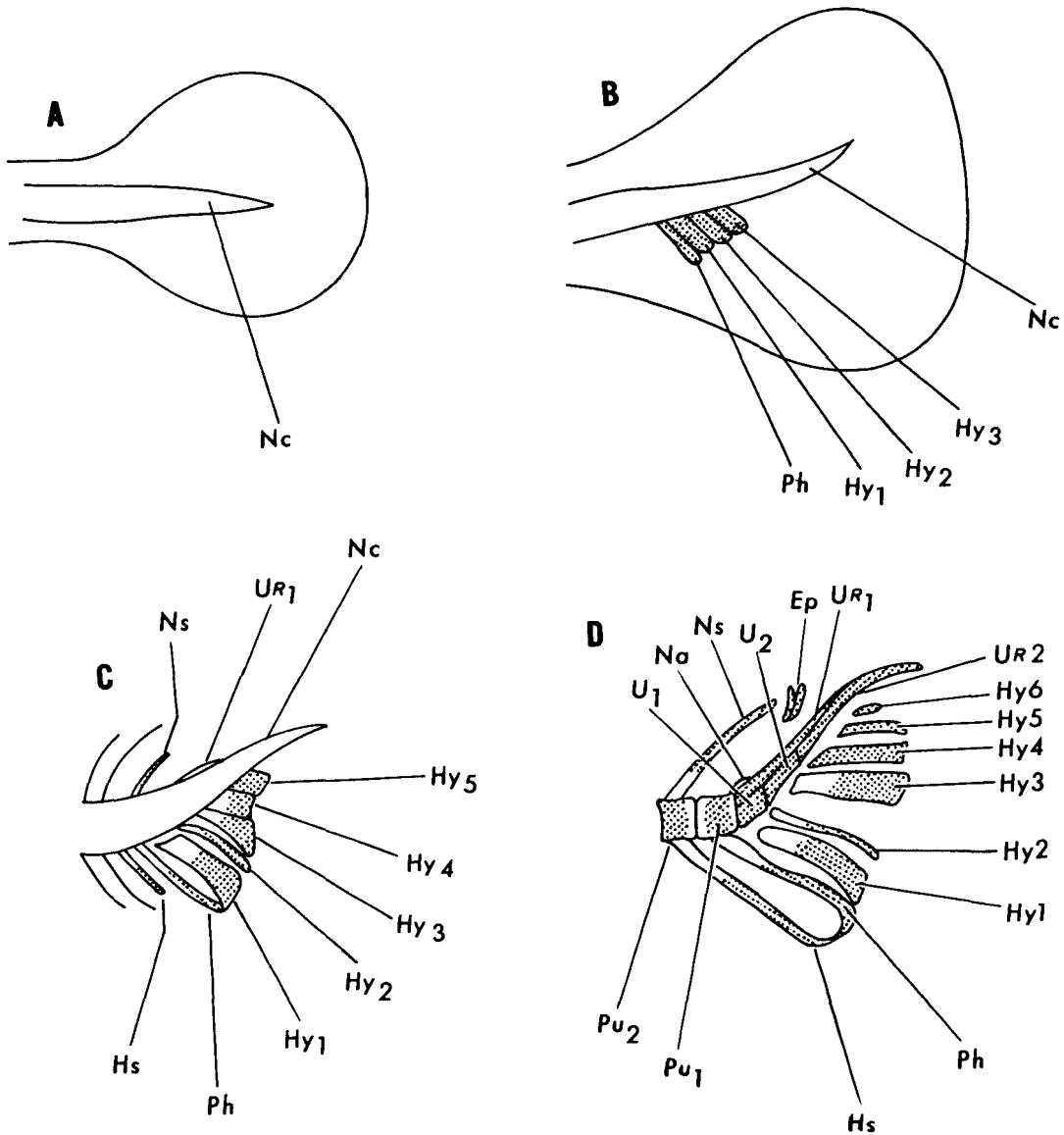


FIGURE 8.—Development of the caudal fin osteology in larval *Alosa sapidissima*. Fin rays are omitted to clearly show support osteology: (A) Early preflexion, 9.2 mm; (B) late preflexion, 10.8 mm; (C) flexion, 13.2 mm; (D) late flexion, 16.9 mm. Hy (1-6) = hypural plates; Ep = epurals; U(1-2) = ural vertebrae; Pu(1-2) = preural vertebrae; Hs = haemal spine; Nc = notochord; Ur(1-2) = uroneurals; Ns = neural spine; Ph = parhypural; Na = neural arch. Clear areas indicate uptake of Alizarin Red S (except for Nc in A, B, and C), while stippled areas indicate uptake of Alcian Blue.

There appears to be a distinct cartilaginous fusion between the haemal spine and the parhypural bones (Fig. 8D).

Postflexion larval and juvenile *A. sapidissima* show complete separation between the ural and preural vertebrae (Fig. 9). The hypurals, neural and haemal spines, neural arch, and the epurals all absorbed Alizarin Red S and Alcian Blue stains. The epurals no longer were fused. The third uroneural was stained

with Alcian Blue. These structures do not appear to completely ossify until well into the juvenile stage of development. A field-sampled specimen 48.0 mm SL showed complete Alizarin Red S absorption in the hypurals, ural and preural vertebrae, and the neural arch. The neural and haemal spines and parhypural exhibited proximal end absorption of Alcian Blue to preural vertebrae 1-4. The two epural bones had absorbed Alcian Blue at both the anterior and posterior

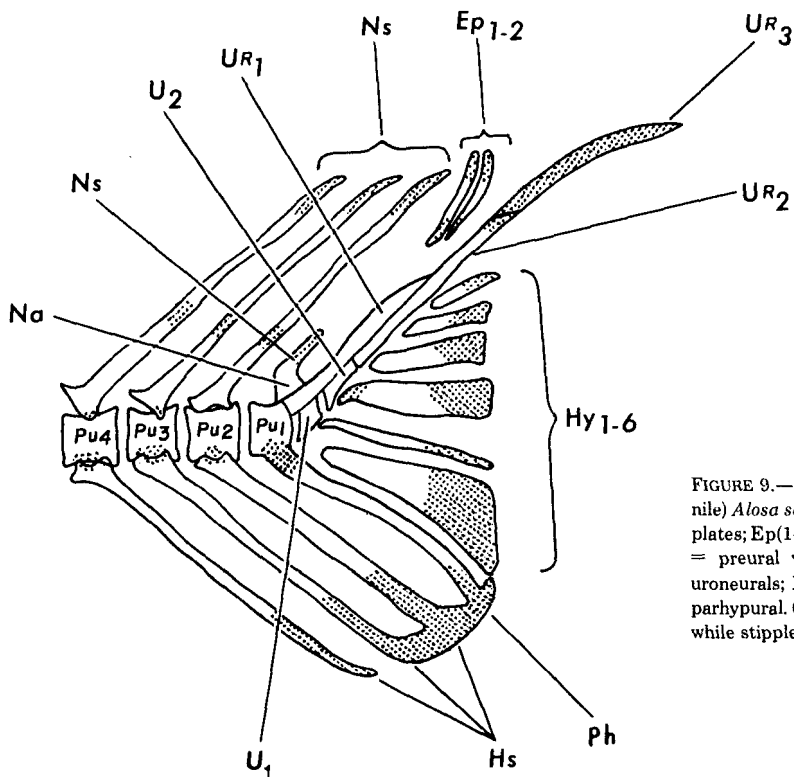


FIGURE 9.—Caudal fin osteology of a postflexion (juvenile) *Alosa sapidissima*, 29.6 mm SL. Hy(1-6) = hypural plates; Ep(1-2) = epurals; U(1-2) = ural vertebra; Pu(1-4) = preural vertebra; Hs = haemal spine; Ur(1-2) = uroneurals; Ns = neural spine; Na = neural arch; Ph = parhypural. Clear areas indicate uptake of Alizarin Red S, while stippled areas indicate uptake of Alcian Blue.

tips of the structures, with Alizarin Red S absorption in the middle.

Pectoral fin development is evident at hatch in the form of a pectoral fin fold and cartilaginous support structures. Incipient pectoral fin rays are also evident in yolk-sac larvae; however, these rays were outlined under light microscopy (25 \times). Development of the pectoral fin appears to be slow when compared with the other fin development characteristics (Table 5). There is a 5.6 mm range of SL over which cartilaginous pectoral fin rays first absorb Alcian Blue stain.

The pelvic fin is the last of the five median and paired fins to start and complete development (Table 5). Pelvic fin development is first evident at the transformation from flexion to postflexion larvae. The pelvic fin basipterygium first appeared during this size interval.

Pigmentation

The distribution of melanophores on *A. sapidissima* appears to be similar to that of other clupeid larvae found in Chesapeake Bay tributaries and the western North Atlantic. There is some variability in the pigmentation patterns among individuals in any given size interval; however, this variation is due in

part to individual chromatophores and melanophores existing in a contracted or expanded state. The specimens illustrated in Figures 10-13 indicate the general pattern of pigmentation typical of the *A. sapidissima* specimens cultured for this study.

Newly hatched *A. sapidissima* have very few melanophores on the snout and over the brain. A newly hatched specimen, 8.2 mm SL, had one stellate melanophore on the tip of the snout and two others in a straight line, spaced at equal intervals, toward the anterior end of the eye. The eyes in this specimen and all the specimens sampled were fully pigmented by 9.5 mm SL (Fig. 10A). Three to five melanophores were present over the brain of a specimen 10.4 mm SL (2 d after hatch). A small but distinct line of melanophores is present above the yolk sac, over the pectoral symphysis and heart, in specimens 9.3-10.5 mm SL (Fig. 10A).

The number of melanophores on the snout and brain increases with increasing SL. A 10.9 mm SL specimen (Fig. 10B) showed an increased number and density of melanophores on the snout. A line pattern of stellate melanophores is developed dorsally from the snout up the midline of the skull and over the top of the brain in larvae 10.9-28.5 mm SL (Figs. 10B-13).

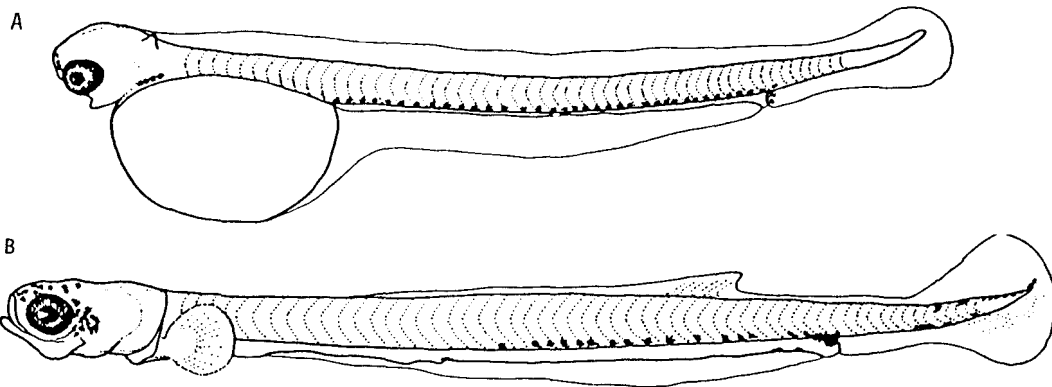


FIGURE 10.—Preflexion *Alosa sapidissima*. A, 9.3 mm SL early preflexion larva; B, 10.9 mm SL late preflexion larva.

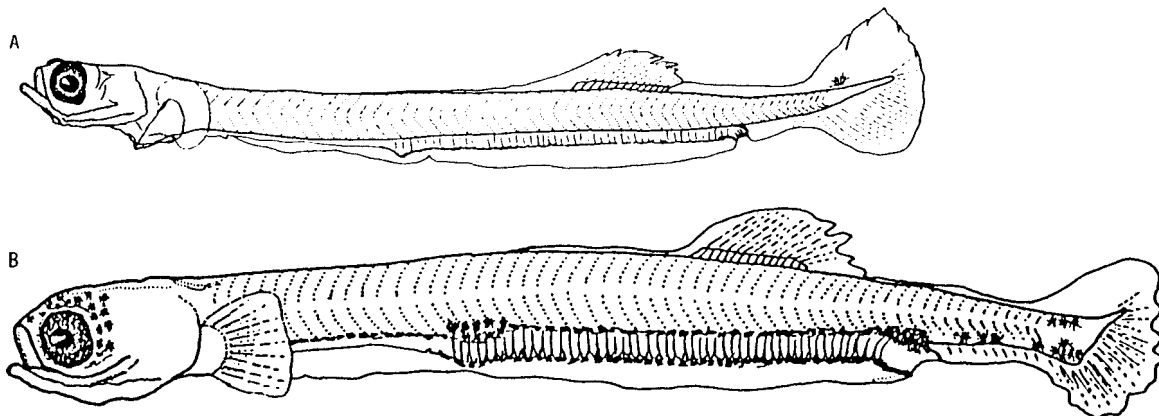


FIGURE 11.—Preflexion *Alosa sapidissima*. A, 12.7 mm SL early flexion larva; B, 15.8 mm SL midflexion larva.

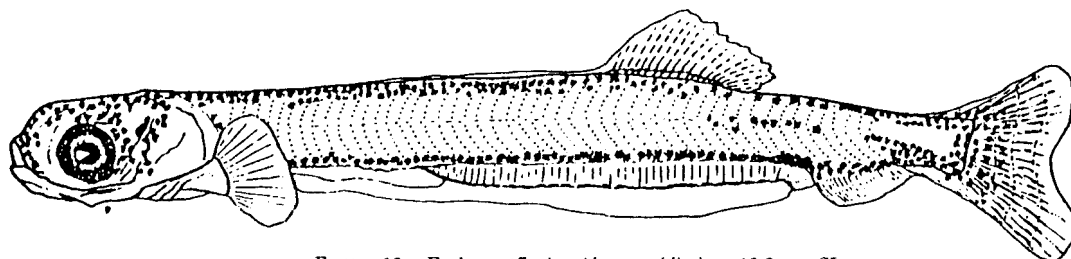


FIGURE 12.—Early postflexion *Alosa sapidissima*, 18.2 mm SL.

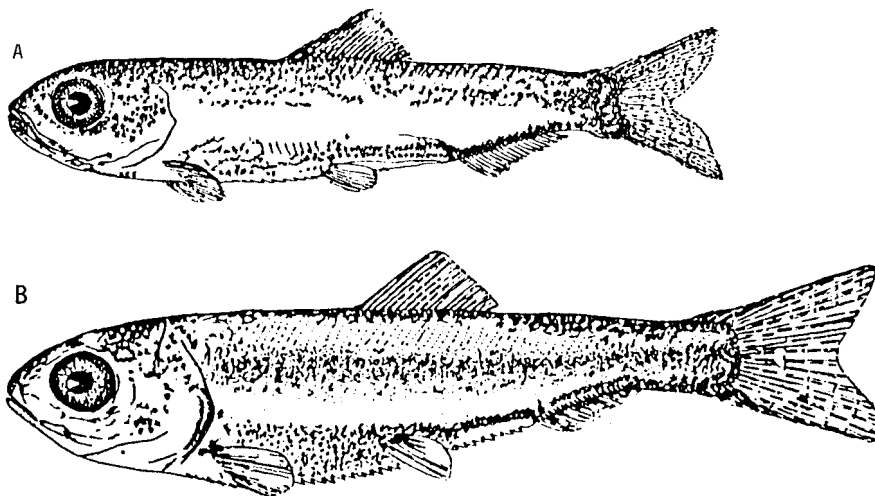


FIGURE 13.—Postflexion *Alosa sapidissima*. A, 23.4 mm SL larva; B, 28.5 mm SL larva.

The pigment pattern associated with the area posterior to the fleshy orbit of the eye, and anterior to the opercular, is variable. The density and number of melanophores around the eye increased to ~22 mm SL. Larvae in the 15-18 mm SL range exhibited most of this pigment just posterior to the fleshy orbit of the eyes, with no melanophores over the opercular bone (Fig. 11). Larvae >20 mm (Fig. 13) exhibited distinct melanophores extending from the fleshy orbit onto the opercular bone. A substantial number of the specimens examined >20 mm SL showed no increase in the actual number of melanophores. Instead, this pigment appeared to migrate, and in some cases contract, from the fleshy orbit of the eye onto the opercular bone. Field-sampled specimens >28 mm showed a reduced number and density of pigment just posterior to the fleshy orbit of the eye and a more concentrated number just anterior to the tip of the opercular bone.

Preflexion *A. sapidissima* have a series of very small, distinct melanophores along the dorsal surface of the gut. These melanophores remained distinct on the larvae to about 18 mm SL (Figs. 10-12). About 2 d after hatch, pigmentation was evident on the ventral surface of the gut. This pigment was in a dense pattern of short dash-shaped melanophores that gave the appearance of a solid line by 15 mm SL (Fig. 11). After 15 mm SL, ventral gut pigmentation contracted from a solid line pattern to a series of spaced melanophores (Figs. 11, 12).

As larvae developed into the postflexion stage, gut pigmentation became increasingly difficult to detect because of the added body tissue and weight. Shortening of the gut, with increasing SL, is seen in con-

junction with the formation of larger, distinct, stellate melanophores along the dorsal gut surface (Fig. 12). There is also a dense concentration of stellate melanophores at the anus in postflexion and juvenile *A. sapidissima*.

Pigment developed along the anal fin base at 15 mm SL where one to three stellate melanophores were found in a series of specimens 15-18 mm SL (Fig. 11). The number of anal fin base melanophores increased to between 14 and 20 for 18-20 mm SL larvae (Fig. 12). Postflexion *A. sapidissima* (Fig. 13) had ~22-26 stellate melanophores in a straight-line pattern over the radials of the anal fin. This line of pigmentation was continuous from the anus, where a dense concentration of melanophores was found, to the caudal peduncle, where pigmentation associated with the caudal fin was evident.

Pigment is found at the base of the dorsal fin over the developing radials in 12 mm SL larvae. From zero to five small dorsal fin melanophores were counted on a series of 11.8-13 mm SL specimens. The number and density of melanophores associated with the dorsal fin increased as the fish grew and the dorsal fin migrated forward. Larvae in the 15-18 mm SL range have 10-19 stellate melanophores over the radials of the dorsal fin (Figs. 11, 12). Larvae >20 mm SL have a stellate melanophore directly over each radial of the dorsal fin (Fig. 13); there are 20 radials with at least one melanophore (more than one in most specimens examined) at the base of the fin.

There is a continuous pair of pigmentation stripes from the eye to the caudal peduncle along the dorsal midline. The paired melanophores anterior to the dorsal fin are distinct, appearing as two lines, while

posterior to the dorsal fin the melanophores are still paired, but coalesce into a single line.

Large stellate melanophores first appear on the posterior end of the lateral line at 18 mm SL (Fig. 12). Between 11 and 15 melanophores are evident during this transition phase between flexion and postflexion larvae. In some of the specimens examined, in the 18-20 mm SL range, pigment was in pairs, one directly above and one directly below the lateral line (Fig. 12). Between 35 and 62 large stellate melanophores were counted on specimens >20 mm SL along the lateral line posterior to the dorsal fin.

Pigment first appeared as very small light chromatophores along the lateral line anterior to the dorsal fin and posterior to the opercular bone in specimens 13-16 mm SL. These cells expanded into distinct stellate melanophores in larger specimens (Fig. 13A). The number of melanophores that could be counted along the lateral line ranged from 7 to 23 in specimens 17.7-21.9 mm SL; more than 50 melanophores were counted for larvae >23 mm SL (Fig. 13). Stellate melanophores in the large postflexion larvae (>25 mm SL) contracted into small indistinguishable melanophores along the lateral line (Fig. 13B).

Newly hatched *A. sapidissima* had no pigment associated with the notochord posterior to the anus (Fig. 10A). Pigment first appeared on the dorsal tip of the notochord at 9.8 mm SL with one to four small melanophores. At 10.9 mm SL (Fig. 10B) pigment was present as eight small melanophores on the dorsal tip and four small melanophores on the ventral tip of the notochord.

Melanophores associated with the caudal region appeared to have migrated toward the anus in larvae 11-13 mm SL. The number and density of melanophores concentrated at the end of the anus increased during this length interval (Fig. 10A). Pigment still appeared in the caudal region as larger, distinct stellate melanophores; however, the number of melanophores remained fairly constant between three and seven for larvae 11-13 mm SL.

Pigment density increased rapidly in the caudal region in larvae >15 mm SL (Figs. 11-13). Melanophores migrated onto the developing caudal rays from the caudal peduncle region, and large stellate melanophores outlined the edge of the caudal peduncle (Fig. 12).

Pigmentation reached its greatest density in larvae 23-25 mm SL (Fig. 13). The number of melanophores increased and became more concentrated in postflexion and juvenile *A. sapidissima*. Larvae >25 mm SL exhibited contraction in size of caudal stellate melanophores, which became difficult to distinguish individually.

DISCUSSION AND CONCLUSIONS

Information pertaining to the morphology of larval *A. sapidissima* presented herein reinforces the summary information presented in Mansueti and Hardy (1967), Lippson and Moran (1974), and Jones et al. (1978). In addition, this study details the ontogenic changes in body development that were previously unavailable in the literature. The earliest studies on *A. sapidissima* larval morphology by Leim (1924) and Hildebrand and Schroeder (1928) reported morphometric body proportions for selected sizes of larvae. Recent studies on the early development of *A. sapidissima* by Watson (1968), Chittenden (1969), and Marcy (1976) presented results that adequately describe the development and ontogenic changes associated with egg and yolk-sac larvae development.

The culture techniques employed in this study (Blair 1976) provided adequate samples to describe the morphological development of *A. sapidissima* over the standard length range that was previously void in the literature (yolk-sac absorption to the postflexion stage). A complete description of morphological development and body proportion ratios is now available from hatch through the adult stage. A combination of this study, Hildebrand (1963), Chittenden (1969), and Marcy (1976), provides a synopsis of the morphology and development of the egg, larva, and adult stages of *A. sapidissima*.

The range of preanal myomeres reported for cultured larval *A. sapidissima* in the present study varies slightly from that previously reported for *A. sapidissima* (Mansueti and Hardy 1967; Lippson and Moran 1974; Jones et al. 1978). Mansueti and Hardy (1967) reported 43-47 preanal myomeres up to 13 mm SL; Lippson and Moran (1974) reported 41-47 between 6 and 14 mm SL; Jones et al. (1978) reported a range of 44-50 ($\bar{x} = 47$) preanal myomeres between 9.0 and 12.9 mm SL. These myomere ranges are lower than those determined in the present study over comparable length ranges (Table 2).

Anterior myomeres can be difficult to discern in *A. sapidissima*, because they are very crowded in the early stages of development (i.e., 8-10 mm SL range). Care was taken in this study to intensify the myomeres by immersing each larvae in glycerin. Berry and Richards (1973) stated that myomere counts can be distorted by crowding in the anterior region; the use of glycerin appears to improve the reliability of myomere counts.

Both this study and that of Mansueti and Hardy (1967) report a decrease in preanal myomere count with ontogeny and shortening of the gut, while main-

taining the same range in total myomere number (Table 2). Jones et al. (1978) did not report a decrease in preanal myomeres with shortening of the gut; rather they indicated an increase in the mean number of preanal myomeres. The information presented by Jones et al. (1978) is based on the work of Chambers et al. (1976), which compares the means and ranges of the preanal myomeres for larval clupeids. Findings of this study and information reported in Mansueti and Hardy (1967) are different from that reported by Chambers et al. (1976). Difference in sample size may explain the difference in results among the studies. Larval *A. sapidissima*, cultured for this study, exhibited a steady decrease in the PAL/SL ratio and in the mean number of preanal myomeres. These changes correspond with shortening of the gut throughout the flexion stage of development.

Ahlstrom (1968) proposed the use of dorsal fin position (PDL), and the relative number of and difference between predorsal myomeres and preanal myomeres, as an accurate method of identifying clupeid larvae. Predorsal myomere counts and ranges reported herein trace the anterior migration of the dorsal fin during ontogeny. The morphometric data in Tables 1 and 2 fulfill the previous information gap in accurate identification of larval *A. sapidissima*.

The sequence of larval fin development and developmental osteology of *A. sapidissima* has not been extensively studied. Bigelow and Welsh (1925) postulated that fin formation may be completed in *A. sapidissima* by 20 mm SL. Nichols (1966) compared the fin ray meristics of several populations of juvenile *A. sapidissima*, and his results compare favorably with this study in the number of fin rays in cultured *A. sapidissima* larvae and juveniles. The mean counts in this study of dorsal (19), anal (21), and pectoral (16) fin rays on cultured larvae and juveniles agree with the means and frequencies of meristic counts made by Nichols (1966) on juvenile *A. sapidissima* from the York River, Va.

Leim (1924), Hildebrand (1963), and Jones et al. (1978) discussed the ventral pigmentation pattern seen from yolk absorption to about 13 mm SL. Indeed, this is one of the most important characteristics in identification of larval *A. sapidissima*. Ahlstrom (1968), however, pointed out that clupeids can be difficult to identify unless precaution is taken to note the sequence of changes in the larva. This is especially true with respect to pigmentation in larval *A. sapidissima*. Leim (1924) and Jones et al. (1978) noted that specimens from freshwater are more heavily pigmented than those in brackish water. This was confirmed in the present study by comparison of field and cultured specimens of larval *A. sapidissima*.

Pigmentation is heavier on the head and dorsal trunk regions of freshwater cultured larvae than on native brackish-water larvae.

The sequence of pigmentation described herein for *A. sapidissima* larvae can be used to identify *A. sapidissima* of freshwater origin, because the culture method utilized freshwater. The pattern of ventral pigment described by Leim (1924) should be used when identifying larvae in the 10-13 mm SL range from samples collected in brackish water. There is a large amount of variability in the distribution of melanophores in freshwater-cultured larvae; therefore, special care should be taken when attempting to identify and confirm larval *A. sapidissima* collected in freshwater. Additionally, meristic characters should be used in conjunction with pigmentation patterns to fully confirm identification of *A. sapidissima* from freshwater samples.

Pigmentation patterns may be useful for separating larval *A. sapidissima* from larval *A. aestivalis* and *A. pseudoharengus*. Leim (1924) used the ventral pigmentation pattern to separate *A. sapidissima* from *A. pseudoharengus*. Chambers et al. (1976) noted that the ventral pattern of pigmentation was similar for *A. aestivalis* and *A. pseudoharengus*. Ventral pigmentation patterns and size differences can be used to distinguish these species when they are in the early preflexion and postflexion stages of development. When *A. sapidissima* is in the early- to midflexion stage and *A. aestivalis* and *A. pseudoharengus* are in the mid- to late-flexion stage, misidentification can occur between these species. Morphometrics presented herein (Tables 1-5) and the work of Chambers et al. (1976) could be used to distinguish these species. Table 6 exhibits the pigmentation characteristics that distinguish larval *A. sapidissima*, *A. aestivalis*, and *A. pseudoharengus*. Careful examination should be made of both the pigmentation patterns (presented in Table 6) and morphometric and meristic characteristics of each of the three species to fully confirm the identification.

ACKNOWLEDGMENTS

There are a number of people to whom we would like to offer thanks for their contributions to this study. Jack Musick, Ken Sulak, Herb Austin, Bill MacIntyre, and Alan Blair (Manager, Harrison Lake National Fish Hatchery, U.S. Fish and Wildlife Service) offered their advice and criticisms. Special thanks also to John J. Govonii for his advice and criticism of this study. John Gourley, John Zernes, Jack Travelstead, and William Kriete helped in the collection of juvenile samples on the Pamunkey

TABLE 6.—Pigmentation summary for larval and juvenile *Alosa sapidissima*, and a comparison of distinguishing pigment characters with *A. aestivalis* and *A. pseudoharengus*.

Development stage and pigment area	American shad, <i>Alosa sapidissima</i>	Blueback herring, <i>Alosa aestivalis</i>	Alewife, <i>Alosa pseudoharengus</i>
Preflexion larvae			
Head region	Eye completely pigmented (9.5 mm SL). 1-9 stellate melanophores on snout (10.72 mm SL); 3-12 stellate melanophores on brain (11.42 mm SL).	Eye completely pigmented (3.1-4.0 mm TL) ¹ .	Slightly pigmented at hatch (>4.82 mm TL) fully pigmented (5.1 mm TL) ² .
Yolk-sac region	4-7 melanophores above yolk sac and over the pectoral symphysis and heart (9.3 mm SL).	Chromatophores scattered on ventral surface of yolk sac ¹ .	Scattered and irregular chromatophores (3-5 mm TL).
Notochord	1-4 melanophores (9.8 mm SL).		
Gut, trunk, and fin region	33-38 small melanophores on dorsal surface of gut (10.9 mm SL).	Irregular chromatophores below pectoral fin; melanophores, some stellate (5.1 mm TL) ¹ ; 4 ventral melanophores below pectoral fin (6.0 mm TL) ¹ .	Transparent at hatch ² ; 2 chromatophores below pectoral; 3-6 posterior to pectoral (3.2-4.8 mm TL), generally sparse and irregular; 2 series of melanophores on each side of ventral line.
Flexion larvae			
Head region	Increased melanophore density over eye, snout, and opercular bone (16-34 stellate melanophores around the eye; 13-15 mm SL).	Increased melanophore density on snout; scattered melanophores on head and operculum (8.8-8.9 mm SL) ⁴ .	Dense scattered melanophores (9.0 mm TL) ³ over snout and between the eyes.
Paired and median fins	1-3 anal fin stellate melanophores (15-18 mm SL). Dorsal fin; 0-5 melanophores (11.8-13 mm SL); 10-19 melanophores (15-18 mm SL).	Double-line pigmentation at pectoral fin (10.4 mm TL) ¹ .	3 melanophores below pectoral fin (6-10 mm TL) ^{1,2} ; melanophores more stellate on caudal fin (9.0 mm TL).
Gut and trunk region	Pigments contract to a solid line after 15 mm SL. Light chromatophores on lateral line (13-16 mm SL).	Small indistinguishable chromatophores on anterior gut; large stellate melanophores on posterior gut (8.8-8.9 mm SL) ⁴ .	12 melanophores on dorsal surface, anterior gut (6 mm TL) ¹ ; 22 melanophores on ventral surface, posterior gut (6 mm TL). ¹ Posterior anus pigmentation generally disappears ² (5-9 mm TL).
Postflexion larvae and juveniles			
Head region	Paired pigment stripes from posterior orbit of eye to caudal peduncle; very heavy pigment around eye (>18.2 mm SL).	Large scattered chromatophores around eye and over snout (20.5 mm TL).	Dense pigment on snout and top of head (29-47.5 mm TL) ¹ .
Paired and median fins	Anal fin: 14-20 stellate melanophores (18-20 mm SL); 22-26 stellate melanophores (23-29 mm SL); >20 dorsal fin melanophores (>20 mm SL).	Large indistinguishable blotches of chromatophores on caudal fin (45 mm TL).	1 large expanded melanophore between pectoral fin bases (15 mm TL) ^{1,2} .
Gut and trunk region	Dense concentration of stellate melanophores at anus; hard to distinguish lateral line; 7-23 melanophores (17.7-21.9 mm SL); >50 melanophores (>23 mm SL).	Defined dorsal rows of melanophores (25.0 mm TL) ¹ .	Chromatophores increasing on dorsal lateral surface between head and caudal fin (19.1-32.2 mm TL) ¹ .

¹Jones et al. (1978).²Cianci (1969).³Chambers et al. (1976).⁴Norden (1980).

River. Bill Twyman, Mike Canada, and Ed Darlington (Harrison Lake National Fish Hatchery, U.S. Fish and Wildlife Service) offered technical assistance and advice on the culture of American shad. Mary Anne Foell drew the figures of the larval fish and offered advice on scientific illustrations. The graphs were drafted by the Rio Blanco Oil Shale Company Drafting Department. Marji Randall, Katie Bechtel, and Judy Rodreick typed the many drafts of this manuscript. Funds for this research were provided by the National Marine Fisheries Service, Northeast Region, through the Anadromous Fish Act (P.L. 89-304).

LITERATURE CITED

AHLSTROM, E. H.

1968. [Book review of] Mansueti, A. J., and J. D. Hardy, Jr., Development of fishes of the Chesapeake Bay region, an atlas of egg, larval, and juvenile stages, Part I. Copeia 1968:648-651.

BERRY, F. H., AND W. J. RICHARDS.

1973. Characters useful to the study of larval fishes. Bur. Commer. Fish., Trop. Atl. Biol. Lab. Contrib. 113, 9 p.

BIGELOW, H. B., AND W. W. WELSH.

1925. Fishes of the Gulf of Maine. Bull. U.S. Bur. Fish. 40(1):1-567.

BLAIR, A. B.

1976. American shad culture and distribution studies at Harrison Lake National Fish Hatchery. Proceedings of the Workshop on American Shad, Amherst, Mass., p. 201-210.

CARSCADDEN, J. E., AND W. C. LEGGETT.

1975. Life history variations in populations of American shad, *Alosa sapidissima* (Wilson), spawning in tributaries of the St. John River, New Brunswick. J. Fish Biol. 7:595-609.

CHAMBERS, J. R., J. A. MUSICK, AND J. DAVIS.

1976. Methods of distinguishing larval alewife from larval blueback herring. Chesapeake Sci. 17:93-100.

CHITTENDEN, M. E., JR.

1969. Life history and ecology of the American shad, *Alosa sapidissima*, in the Delaware River. Ph.D. Thesis, Rutgers univ., New Brunswick, N.J., 471 p.

CIANCI, J. M.

1969. Larval development of the alewife, *Alosa pseudo-*

- harengus*, and the glut herring, *Alosa aestivalis*. M.S. Thesis, Univ. Connecticut, Storrs, 62 p.
- DINGERKUS, G., AND L. D. UHLER.
1977. Enzyme clearing of alcian blue stained whole small vertebrates for demonstration of cartilage. *Stain Technol.* 52:229-232.
- HILDEBRAND, S. F.
1963. Family Clupeidae. Genus *Alosa*. In Y. H. Olsen (editor), *Fishes of the western North Atlantic*, part 3, p. 293-312. *Mem. Sears Found. Mar. Res.*, Yale Univ., Vol. 1.
- HILDEBRAND, S. F., AND W. C. SCHROEDER.
1928. Fishes of Chesapeake Bay. *Bull. [U.S.] Bur. Fish.* 43:1-388.
- HOUDE, E. D., W. J. RICHARDS, AND V. P. SAKSENA.
1974. Description of eggs and larvae of scaled sardine, *Harengula jaguana*. *Fish. Bull.*, U.S. 72:1106-1122.
- JONES, P. W., F. D. MARTIN, AND J. D. HARDY, JR.
1978. Family Clupeidae: *Alosa sapidissima*. In *Development of fishes of the mid-Atlantic Bight*, Vol. 1, p. 98-104. U.S. Dep. Inter., U.S. Fish Wildl. Serv.
- LEIM, A. H.
1924. The life history of the shad (*Alosa sapidissima* (Wilson)) with special reference to the factors limiting its abundance. *Contrib. Can. Biol. New Ser.* 2:161-284.
- LIPPSON, A. J., AND R. L. MORAN.
1974. Manual for identification of early developmental stages of fishes of the Potomac River estuary. *Md. Dep. Nat. Resour.*, Baltimore, 282 p.
- MANSUETI, A. J., AND J. D. HARDY, JR.
1967. Development of fishes of the Chesapeake Bay region; an atlas of egg, larval, and juvenile stages, Part 1. *Nat. Resour. Inst.*, Univ. Md., 202 p.
- MARCY, B. C., JR.
1976. Early life history studies of American shad in the lower Connecticut Yankee plant. In D. Merriman and L. M. Thorpe (editors), *The Connecticut River ecological study*. *Am. Fish. Soc. Monogr.* 1:141-168.
- MOSER, H. G., AND E. H. AHLSTROM.
1970. Development of lanternfishes (family Myctophidae) in the California current. Part I. Species with narrow-eyed larvae. *Bull. Los Ang. Cty. Mus. Nat. Hist. Sci.* 7, 145 p.
- NICHOLS, P. R.
1966. Comparative study of juvenile American shad populations by fin ray and scute counts. *U.S. Fish Wildl. Serv., Spec. Sci. Rep. Fish.* 525, 10 p.
- NORDEN, C. R.
1980. Morphology and food habits of the larval alewife, *Alosa pseudoharengus* (Wilson) in Lake Michigan. *Conf. Great Lakes Res.* 10:70-76.
- RICHARDS, W. J., R. V. MILLER, AND E. D. HOUDE.
1974. Egg and larval development of the Atlantic thread herring, *Opisthonema oglinum*. *Fish. Bull.*, U.S. 72:1123-1136.
- SCOTT, W. B., AND E. J. CROSSMAN.
1973. Freshwater fishes of Canada. *Bull. Fish. Res. Board Can.* 184, 966 p.
- SOKAL, R. R., AND F. J. ROHLF.
1969. Biometry. *The principles and practice of statistics in biological research*. W.H. Freeman, San Franc., 776 p.
- TUCKER, J. W., JR.
1978. Larval development of four species of bothid flatfish in the *Citharichthys-Etropus* complex: *C. Cornutus*, *C. Gymnorphinus*, *C. Spilopterus*, and *E. Crossotus*. Masters Thesis, North Carolina State Univ., Raleigh.
- WATSON, J. R.
1968. The early life history of the American shad, *Alosa sapidissima* (Wilson), in the Connecticut River above Holyoke, Massachusetts. Masters Thesis, Univ. Mass., Amherst.